Published in final edited form as:
Biomaterials. 2011 January ; 32(2): 587–597. doi:10.1016/j.biomaterials.2010.08.106.

An injectable thiol-acrylate poly(ethylene glycol) hydrogel for sustained release of methylprednisolone sodium succinate

Christopher D. Pritchard[a,*], **Timothy M. O'Shea**[b], **Daniel J. Siegwart**[a], **Eliezer Calo**[c], **Daniel G. Anderson**[a], **Francis M. Reynolds**[d], **John A. Thomas**[e], **Jonathan R. Slotkin**[e], **Eric J. Woodard**[f], and **Robert Langer**[a,b]

[a]Department of Chemical Engineering, Massachusetts Institute of Technology, Cambridge, MA 02139, USA

[b]Harvard-MIT Division of Health Sciences and Technology, Massachusetts Institute of Technology, Cambridge, MA 02139, USA

[c]Koch Institute for Integrative Cancer Research, Massachusetts Institute of Technology, Cambridge, MA 02139, USA

[d]InVivo Therapeutics Corporation, Cambridge, MA 02142, USA

[e]Department of Neurosurgery, The Washington Brain and Spine Institute, Washington, DC 20010, USA

[f]Department of Neurosurgery, New England Baptist Hospital, Cambridge, MA 02120, USA

Abstract

Clinically available injectable hydrogels face technical challenges associated with swelling after injection and toxicity from unreacted constituents that impede their performance as surgical biomaterials. To overcome these challenges, we developed a system where chemical gelation was controlled by a conjugate Michael addition between thiol and acrylate in aqueous media, with 97% monomer conversion and 6 wt.% sol fraction. The hydrogel exhibited syneresis on equilibration, reducing to 59.7% of its initial volume. It had mechanical properties similar to soft human tissue with an elastic modulus of 189.8 kPa. Furthermore, a mesh size of 6.9 nm resulted in sustained release of methylprednisolone sodium succinate with a loading efficiency of 2 mg/mL. Functionalization with 50 μg/mL of an oligolysine peptide resulted in attachment of freshly isolated murine mesenchymal stem cells. The rational design of the physical, chemical and biological properties of the hydrogel makes it a potentially promising candidate for injectable applications.

Keywords

Cell adhesion; Controlled drug release; Hydrogel; Peptide; Polyethylene oxide; Spinal surgery

[*]Corresponding author. Department of Chemical Engineering, Massachusetts Institute of Technology, Room E25-342,45 Carleton St., Cambridge, MA 02142, USA. Tel.: +1 212 729 8988; fax: +1 617 258 8827. cpritcha@mit.edu (CD. Pritchard).

1. Introduction

Synthetic polymeric hydrogels represent a promising technology platform for therapeutic intervention in a wide range of diseases and traumatic injuries. Comprising a three-dimensional insoluble polymer network formed through the covalent or physical crosslinking of hydrophilic macromer precursors, hydrogels thermodynamically interact with aqueous media in a similar way to the native extracellular matrix (ECM). Owing to their easily tunable physical and chemical properties, hydrogels have been explored in a variety of diverse biomedical applications across the domains of controlled drug delivery, in vitro disease modeling and regenerative medicine [1–3]. Poly(ethylene glycol) (PEG)-based hydrogels are particularly attractive for rapid clinical translation because devices and delivery systems based on PEG already have FDA approval due to the characteristic properties of PEG that limit non-specific protein adhesion and cellular interactions [4]. To date, a wide variety of PEG-based hydrogels has been fabricated using numerous covalent gelation mechanisms. These include the free radical chain growth homopolymerization of activated -enes (most notably acrylates) [5]; free radical step-growth photopolymerization of thiols and -enes [6–8], click chemistry of alkynes and azides [9], and conjugate Michael addition of multifunctional thiol and activated -ene precursors [10,11]. Incorporation of various biological, chemical and/or mechanical cues has allowed these biomaterials to be applied to the study of cellular matrix interactions as well as disease states in vitro by recreating intricate cellular microenvironments [12]. However, the suitability of some of these systems for in situ gelation is limited by incomplete conversion of reactive functional groups and high sol fraction [2]. In addition, the use of metal catalysts, or photoinitiators and ultraviolet (UV) light, to initiate and propagate gelation creates biocompatibility concerns [9,13]. Additional structural constraints, caused by substantial network defects and problematic large equilibrium volume swelling, have also hampered in vivo material performance in the past. Duraseal,a hydrogel composed of a mixture of polyethylene glycol (PEG) ester and trilysine amine solutions, caused spinal cord compression due to undue swelling and as a result induced or worsened quadriparesis requiring intervening decompression surgery [14,15]. Hydrogels of co-poly(methylacrylate-hydroxyethyl acrylate) used in scleral buckling procedures to treat retinal detachment displayed compromised long-term performance attributed to undesirable swelling and also degradation [16,17]. These cases demonstrate that unfavorable physical properties of injectable hydrogels can create severe post-surgical complications. Such limitations have been overcome by post-gelation processing prior to implantation, but this precludes their surgical application via a minimally invasive injection [18]. Hydrogels that display temperature dependent de-swelling properties have been developed previously through the covalent crosslinking of thermoreversible physical gels composed of triblock poly (ethylene oxide) (PEO)and poly(propylene oxide) (PPO) macromers. However a capacity to achieve sustained release of low molecular weight molecules using this system was not demonstrated and photopolymerization was still required for irreversible network formation [19].

We were interested in developing a more robust hydrogel technology platform that could overcome the above constraints and bypass additional processing requirements through a capacity to safely transition from a sol precursor mixture to a gel state *in situ*. Utilizing a

rational engineering design approach, we defined performance parameters applicable to a wide spectrum of diseased and injured tissues prior to the selection of material constituents and a gelation mechanism. These requirements included no volume increase during equilibration, resilient mechanical properties that match human tissues of interest, a mesh size adequate for diffusion-controlled release of hydrophilic small molecule drugs, tunable gelation kinetics and the ability to functionalize the material with biological motifs to guide cellular interactions. An injectable biomaterial displaying such properties would provide a substrate for diverse therapeutic interventions that could permit minimally invasive surgical application, minimal compressive tissue damage, reduced inflammation and risk of infection, as well as faster recovery for patients following surgery [20]. Given the desire to achieve rapid gelation under ambient conditions without use of reaction initiators or UV light, conjugate thiol-ene Michael addition was selected as a suitable chemical crosslinking mechanism for the injectable hydrogel system. This reaction involves the direct addition of a dissociated thiolate nucleophile and an unsaturated carbon double bond, activated by a neighboring electron withdrawing group such as an ester or amide [10,11,21,22]. Advantageously, this mechanism has been shown to be applicable to a wide range of commercially available precursors, forms polymer networks with minimal structural deficiencies and can react completely within a surgically relevant timeframe, while avoiding the production of free radicals [23]. This paper describes the rational design and characterization of a PEG-based hydrogel and an investigation of its applicability for drug release and cell adhesion in vitro.

2. Materials and methods

2.1. Materials

Poly(ethylene glycol) diacrylate (PEG-400-DA, Polyscience, Warrington, PA) and ethoxylated trimethylolpropane tri-3-mercaptopropionate (ETTMP, Thiocure 1300, Bruno Bock, Marschacht, Germany) were passed through a short column of activated basic aluminum oxide (ColeeParmer Instrument Company, Vernon Hills, IL) to remove the radical inhibitor, hydroquinone monomethyl ether (MEHQ, 400 ppm) prior to use. Physiologically isotonic phosphate-buffered saline (PBS, pH 7.4, 1.06 mM potassium phosphate monobasic, 155.17 mM sodium chloride, 2.97 mM sodium phosphate dibasic, Invitrogen, Carlsbad, PA), Dulbecco's Modified Eagle Medium (DMEM, 1X, 4.5 g/L Glucose, 4 mM L-glutamine, Invitrogen, Carlsbad, PA), methylprednisolone sodium succinate (MPSS, CAS 2375-03-3, SigmaeAldrich Corp., St. Louis MO), oligolysine peptide (14 lysine amino acid units with a cysteine at both the N and C termini, Applied Biosystems 430A, Biopolymers & Proteomics Core Facility, Koch Institute at MIT, Cambridge MA), sodium hydroxide (NaOH, Mallinckrodt), and poly(ethylene glycol) (400 g/mol, Fluka), acetonitrile (Chromasolv Plus, Sigma–Aldrich Corp., St. Louis MO), ddH_20 (NANOpure, Thermo Fisher Scientific, Waltham MA), and formic acid (Sigma–Aldrich Corp., St. Louis MO) were used as received.

2.2. Instrumentation

UV–vis was measured on a Spectramax Plus spectrophotometer (Molecular Devices). pH was measured using a digital pH probe (Russell RL060P, Thermo Scientific). Fourier

transform infrared (FT-IR) spectroscopy was taken using an Alpha FT-IR with Eco ATR sampling module (Bruker Optics, Billerica MA). Dynamic rheology was performed using an AR G-2 with a 40 mm diameter 2° cone and plate set-up (TA Instruments, New Castle, DE). Specific gravity was measured using a kit (Mineralab, Prescott AZ). Tensile testing was performed on a Model 5542 (Instron, Norwood, MA). High performance liquid chromatography (HPLC) was performed on an Agilent 1100 (Agilent Technologies Inc., Santa Clara CA) based on an existing procedure [24]. A C18 column (dC18 Atlantis 5 μm, 4.6 mm × 250 mm, Waters, Ireland) was used at a flow rate of 1 mL/min. The mobile phase was 60:40 acetonitrile and ddH20 with 0.1% formic acid. Mathematica (Mathematica, Wolfram Research, Champaign IL) was employed. Microscopy was performed on using a Carl Zeiss microscope (MicroImaging Inc., Thornwood NY).

2.3. Poly(ethylene glycol) hydrogel fabrication

Poly(ethylene glycol)-based hydrogels were formed using precursors containing multiple thiol and acrylate functional groups capable of reacting in an aqueous solvent to form a network structure (Fig. 1 and Scheme 1). Aqueous stock solutions of the two precursors, PEG-400-DA, and ETTMP, were prepared by dissolving the polymers in PBS at 4 °C for 24 h. To fabricate the hydrogels, appropriate volumes of the two stock solutions resulting in an equimolar stoichiometric ratio of thiol and acrylate functional groups were combined, yielding a final total polymer concentration of 25 wt.% in a Falcon tube at 4 °C. Following a 5 min incubation period at 4 °C to increase dissolution of the precursors in the mixture, molds of a desired size were filled with the solution and transferred to an incubator at 37 °C to complete gelation. Gelation occurred within 5 min of incubation. However, samples produced for structural characterization and mechanical testing were maintained in the 37 °C environment for 20 min to promote complete conversion of functional groups. The gelation protocol described above was applied to all hydrogels prepared in PBS. For cell culture studies, DMEM was incorporated as the solvent phase in the hydrogel by incubating the cured hydrogel in the media for a 24 h period, prior to cell seeding. For MPSS encapsulation and release studies, weighed samples of the steroid were incorporated into the PEG-400-DA solution for a final concentration of 0.5,1 or 2 mg/ mL in the hydrogels. Functionalization of the hydrogel with an oligolysine peptide was performed by dissolving the peptide in the PEG-400-DA in solution, prior to mixing with the ETTMP stock solution. The oligolysine was reacted into the hydrogel via its thiol-containing cysteine end residues. Solutions were sterilized by syringe filtration through a 0.2 μm nylon filter. The concentrations of oligopeptide used were 5, 50 and 500 μg/mL.

2.4. Hydrogel precursors analysis

2.4.1 Solubility of hydrogel precursors—To investigate the parameters affecting solubility of ETTMP in PBS, nine standard solutions, with concentrations from 5 wt.% to 45 wt.%, at 5 wt.% increments, were prepared and stored at 4 °C for 24 h. Following vortexing, 4 × 200 μL of each standard was aliquotted into a transparent 96-well plate and equilibrated at 4 °C for 30 min. The absorbance of the standards was then assessed spectrophotometrically at 37 °C for 20 min (λ = 450 nm). The initial absorbance and the time at which a rapid increase in absorbance occurred (represented by a characteristic inflection in the absorbance curve) were used as measures of solubility at 4 °C and stability

(precipitation/phase separation) at 37 °C respectively. The solubility of the PEG-400-DA was assessed but not reported in this paper, as this polymer was soluble over the concentration and temperature ranges of interest.

2.4.2. Measuring the pKa of ETTMP—A 50 mL 0.1 M (0.3 N) solution of ETTMP in ddH_20 was prepared in a 250 mL beaker with a magnetic stir bar and a digital pH probe. A 0.1 M solution of NaOH in ddH20 was titrated in increments of 500–1200 μL into the ETTMP solution with concomitant pH measurements until the pH increased beyond the upper equivalence point (approximately 150 mL). The pKa was determined as the pH halfway between the equivalence points.

2.5. Gelation kinetics and mechanism

The gelation kinetics involving sol–gel transition and chemical conversion were assessed using dynamic rheology and FT-IR spectroscopy respectively. The Michael addition mechanism was assessed by evaluating the gelation response as a function of buffer pH and counterion content using these two tests. To study the presence of radical reactions (thiyl-acrylate addition or acrylate homopolymerization), gelation was also performed in the presence of radical inhibitor, MEHQ, by not filtering PEG-400-DA prior to use.

2.5.1. FT-IR analysis—500 μL hydrogel discs were cast using a 24-well tissue culture plate as a mold following the fabrication protocol outlined above. Hydrogel samples were extracted from their molds after curing and either lyophilized for a period of 36 h, or equilibrated by incubation at 37 °C in a 12-well plate (4 mL per well of PBS) for 48 h followed by lyophilization. FT-IR spectra were obtained on the dry gels by measuring attenuated total reflection. The differences in the amount of unreacted acrylate and thiol constituents remaining in the two hydrogel sample groups (characterized by C=C stretch at 1675–1600 cm^{-1} and S–H stretch at 2550–2600 cm^{-1}) were assessed through a quantification analysis using the OPUS software package. Standard curves for the quantification analysis were constructed by diluting the precursors to known concentrations using poly(ethylene glycol) (400 g/mol) polymer. Linear regression curves were constructed from this data and used to assess residual acrylate (R^2 = 0.998) and thiol (R^2 = 1.000) in the hydrogels.

2.5.2. Dynamic rheology—The sol–gel transition was studied *in situ* using dynamic rheology. 600 μL aliquots of precursor/PBS solution were prepared and incubated at 4 °C for 5 min. The solutions were then transferred to the rheometer. First measurements were recorded 40 s after removal from the 4 °C environment. The dynamic evolution of the mechanical properties (storage (G') and loss (G'') moduli) was assessed at 5% strain and a frequency of 10 rad s^{-1} for 10 min. Separately, a frequency sweep was performed at 5% strain to verify that testing conditions were within the linear viscoelastic range. The gel point was characterized as the time when $\tan(\delta) = G''/G' = 1$ was observed, which was deemed a valid approximation given that the prepared hydrogel was stoichiometrically balanced and sufficiently far away from its glass transition temperature [25,26]. The proposed mechanism of hydrogel formation via a base catalyzed Michael type addition reaction between thiolate anion and acrylate was studied further by assessing functional group conversion and gelation

kinetics under varying buffer conditions. Potassium and sodium phosphate buffer 0.1 M solutions with pH values of 6,6.6,7,7.4 and 8 were prepared by mixing and diluting appropriate quantities of 1 M solutions containing their respective monobasic dihydrogen and dibasic monohydrogen phosphate salts. Additional FT-IR and dynamic rheology experiments were performed on hydrogels using these buffer solutions as the solvent phase. The extent of chemical conversion of the acrylate and thiol functional groups and the gel point time were characterized for each buffer solution. For dynamic rheology testing of these hydrogels, the 5 min incubation procedure at 4 °C was not necessary.

2.6. Structural and mechanical properties of the hydrogel

2.6.1 Hydrogel equilibration and sol fraction—The hydrogel equilibration behavior and sol fraction were evaluated using 500 μL hydrogel discs prepared in a 24-well plate mold. The wet masses of hydrogels cured and swollen for 6, 12, 24, 48 and 72 h were recorded before then being lyophilized to determine the mass of dry polymer. To calculate the relaxed (immediately after curing) and equilibrium polymer volume fractions ($v_{2,r}$ and $v_{2,s}$ respectively, per equations (1) and (2)), the specific gravity of the hydrogel (cured and equilibrated for the same above incremental time points) as well as the dry polymer network were measured, using a specific gravity kit and applying Archimedes' buoyancy law before then being converted to volume measurements.

$$\text{Equilibrium polymer volume fraction} v_{2,s} = \frac{V_p}{V_{hgel,s}} \quad (1)$$

$$\text{Polymer volume fraction in the relaxed state} v_{2,r} = \frac{V_p}{V_{hgel,r}} \quad (2)$$

The sol mass fraction was computed by comparing the differences in dry polymer weight between the cured and equilibrated samples.

2.6.2. Hydrogel degradation—Individual 500 μL hydrogel discs were incubated in 4 mL PBS in 12-well plates for a period of 12 weeks to assess hydrolytic degradation. Masses of wet and lyophilized gels were measured in triplicate at 1, 2, 4, 6, and 9 weeks. Before lyophilization, the hydrogels were washed in distilled water to remove any residual salt that may have built up on the surface. The total dry polymer mass loss of each sample was determined through comparisons with the dry weight of cured (nonequilibrated) samples.

2.6.3. Mechanical testing of equilibrated and cured hydrogels—To assess the mechanical properties of the hydrogel, tensile testing was performed on cured and equilibrated samples. Planar sheets of hydrogel with 3 mm uniform thickness were fabricated in a flat rectangular mold, with equilibrated samples incubated in PBS for 48 h before use. Immediately prior to testing, ASTM 412-D type specimens were cut from the planar sheet using a stainless steel die and a mallet. The final dimensions of the specimen were measured using Vernier calipers before being loaded into the testing jig. Tests were performed using a 50 N static load cell under a strain rate of 5 mm min^{-1}. The shear and

elastic modulus were computed assuming incompressible neo-Hookean mechanics (Poisson's ratio, $v \sim 0.5$) and assessing engineering stress as a function of both extension ratio and deformation factor [27,28]. Using a statistical mechanics approach and applying the experimentally observed modulus value (G) (as calculated by fitting a linear regression for engineering stress versus deformation factor), the number of elastically effective chains per unit volume (v_e/V_o) for equilibrated hydrogels was determined (Equation (3)).

$$\tau = \left[RT \left(\frac{v_e}{V_o} \right) \left(\frac{v_{2,s}}{v_{2,r}} \right)^{1/3} \right] \left(\lambda - \frac{1}{\lambda^2} \right) \Rightarrow v_e = v \left(1 - \frac{2N}{v} \right) \; G_{aff} = RT \left(\frac{v_e}{V_o} \right) \left(\frac{v_{2,s}}{v_{2,r}} \right)^{1/3} = \frac{1}{3} E \quad (3)$$

Additional modeling of the gel structure through the application of the Miller-Macosko branching theory for end-linked networks was used to characterize the extent of reaction, as well as the ideal mechanical properties based upon the measured sol fraction [29,30]. An approximate mesh size for the hydrogel in both cured and equilibrium states was also determined by calculating the distance between active crosslinks, μ_e ($=2v_e/f$).

2.7. In vitro analysis

2.7.1. Drug release and stability study—The release kinetics of MPSS from hydrogels were studied as follows. Hydrogels containing 0.5, 1 and 2 mg/mL MPSS (dissolved in precursor solutions prior to gelation) were fabricated in 1.7 mL Eppendorf tubes (21 × 250 μL for each concentration of MPSS). Following complete gelation (20 min at 37 °C), 1 mL PBS was added to each tube and incubated at 37 °C. Degradation of MPSS in PBS was measured by incubating stock solutions of MPSS in PBS at 37 °C (500, 250 and 125 μg/mL, 21 × 1 mL for each concentration). After 6,12, 24,48, 96,192 or 384 h the solution above the hydrogels or from stock aliquots were extracted and stored in Eppendorf tubes at −80 °C (n = 3 for each concentration at each time point). MPSS concentrations were analyzed using high HPLC based on an existing procedure [24]. Ultraviolet light absorbance was measured at 238 nm. The MPSS peak elutes at 4.864 min. A standard curve was calculated using HPLC peak areas from six points in a series dilution from a stock solution (85 μg/mLMPSS in PBS, diluted geometrically. A response factor of 8.7446 mAUs mL μg^{-1} was calculated with R^2 of 0.9997 (linear regression with zero intercept). Mass transfer coefficients for MPSS release from the hydrogel were calculated by solving a system of differential equations for drug release kinetics and the degradation of MPSS in PBS and fitting a regression of appropriate form to the data using Mathematica.

2.7.2. Cell adhesion assay—Hydrogels were prepared in PBS, with final concentrations of oligolysine peptide of 0, 5, 50 and 500 μg/mL (4 × 250 μL each), in a sterile 24-well polystyrene tissue culture plate, before being incubated in DMEM for 24 h to facilitate solvent exchange. On the same plate, 4 wells were incubated with 200 μL for 3 h at room temperature, with 0.25 mg/mL oligolysine peptide in DMEM, followed by aspiration of the media. The remaining 4 wells were left uncoated as positive controls. The tissue culture plate was further sterilized in a laminar flow hood by ultraviolet irradiation for 15–30 min with the addition of excess media to the gels to maintain hydration. Freshly isolated bone marrow derived murine mesenchymal stem cells (mMSC) were then seeded using sterile

technique at a density of 10^5 cells per well and incubated (2 mL DMEM per well, 37 °C, 5% CO2). After 24 h, digital images of the cells were obtained from all wells (40× Phase 2 contrast bright field, light microscope).

2.8. Statistics

Throughout this paper all statistics are represented as mean ± standard deviation. Hypothesis tests of comparison were performed using the student's t-test, assuming that variances were unknown and not equal, with *p*-values of less than 0.05 taken as significant.

3. Results

3.1. Hydrogel precursor analysis

3.1.1. Solubility of ETTMP—PEG-DA-400 was soluble in PBS over the temperature (4–37 °C) and concentration (5–45 wt.%) ranges of interest. In contrast, the solubility of ETTMP in PBS changed as a function of concentration. Therefore, experiments were performed to characterize the solubility of ETTMP in PBS at 4 °C (Fig. 2) and stability during heating from 4 to 37 °C (Fig. 3). ETTMP solubility in PBS at 4 °C decreased non-linearly from 5 to 25 wt.%, determined by the increasing absorbance of visible light (λ = 450 nm). The solubility of the polymer then increased again from 25 to 45 wt.%, exhibiting the highest solubility from 40 to 45 wt.% (Fig. 2). The results were confirmed by visual inspection, where mixtures from 20 to 35 wt.% were above their cloud point at 4 °C in PBS. The stability of ETTMP in PBS when heated from 4 to 37 °C was measured by dissolving ETTMP at different concentrations at 4 °C, followed by heating at 37 °C for 20 min. These experimental conditions were chosen to replicate the physiological environment under which gelation would take place *in situ*. Regression of error functions (in the form $A \text{ erf } [b(t - t_{inf})] + d$) was applied to the temporal absorbance profiles and used to determine the time where the inflection in absorbance of visible light (λ = 450 nm) occurred (t_{inf}), marking the maxima in rate of precipitation (Fig. 3). The precipitation time decreased from approximately 794—485 s between 5 and 10 wt.%. Precipitation time increased again markedly from 483 to 1044 s to between 20 and 45 wt.%. Based on these results, gelation experiments were performed with varying concentrations of ETTMP in the stock solution. The concentration of the PEG-400-DA stock solution was modified accordingly to maintain a total polymer concentration of 25 wt.% in the hydrogels, with no precipitation of PEG-400-DA observed in the stock solution over the resulting concentration range. Higher sol fractions of the resulting hydrogels were observed using ETTMP stock solutions between 25 and 35 wt.% compared to 40 wt.%, associated with reduced ETTMP stability in solution. Gelation did not readily occur using a 45 wt.% ETTMP stock solution. When the concentration was increased above 50 wt.%, the mixing was greatly reduced due to increased viscosity, which hindered the polymerization. The 40 wt.% concentration was therefore used for further experiments.

3.1.2. Measuring the pK_a of ETTMP—The pK_a of ETTMP was measured in order to predict the extent of thiol deprotonation as a function of pH in aqueous media. A titration of 0.1 M ETTMP at 24 °C with 0.1 M NaOH resulted in a pK_a for ETTMP of 9.87 (Fig. 4).

3.2. Gelation kinetics

3.2.1. Fourier transform infrared spectroscopy—Attenuated total reflection FT-IR was used to measure PEG-400-DA acrylate C=C stretch (1675–1600 cm^{-1}) and ETTMP S–H stretch (2550–2600 cm^{-1}) (Fig. 5). Following the reaction in PBS, 15.0 vol.% thiol and 6.7 vol.% acrylate were detected in cured gels, after lyophilization. 8.0 vol.% thiol and −2.7 vol.% acrylate were detected in equilibrated gels, after lyophilization. These parameters were determined using the FT-IR quantification software. The apparatus used appeared to have a detection limitation for low macromer concentrations, where peaks expected based on the values obtained could not clearly be distinguished from noise (Fig. 5C and D).

3.2.2. Dynamic rheology—Dynamic rheology was performed to quantify the critical gelation time, defined where the magnitudes of the elastic (G') and loss (G'') moduli are equivalent (Fig. 6). Gelation times were measured in phosphate buffer solutions of varying pH and either Na or K cations. The gelation time decreased exponentially with increasing pH, for 0.1 M phosphate buffer solution containing either Na or K cations (Fig. 7). The gelation time was also weakly dependent on the cation in the buffer, decreasing as the ionization energy of the cation decreased from Na to K. The gelation time in PBS increased with the inclusion of MEHQ, from 459.7 to 475.3 s ($p < 0.05$).

3.3. Structural and mechanical properties of the hydrogel

3.3.1. Hydrogel equilibration and sol fraction—Equilibrium polymer volume, mass and sol fractions were measured for hydrogels cured at 37 °C in different solvents. The hydrogel exhibited syneresis during equilibration. The polymer volume and mass fractions in the relaxed state were 22.1 vol.% and 26.1 wt.% immediately post-gelation and increased to 36.7 vol.% and 39.4 wt.% after 12 h of incubation in PBS. This equilibrium value was maintained relatively constant through 48 h (Fig. 8). The polymer mass fraction followed the volume fraction profile over the 72 h period analyzed but was offset by 2–3% at each time point. By comparing dry mass initially and following equilibration, it was determined that 93.7 ± 1.0 wt.% and 95.4 ± 1.4 wt.% of the polymer precursors were incorporated into the hydrogel network in PBS with or without MEHQ respectively (no statistical significance). MEHQ did not affect the equilibrium volume or mass fractions. Hydrogels prepared in ddH_20 without MEHQ incorporated 64.2 ± 5.8 wt.% of precursors into the gel network and had an equilibrium polymer mass fraction of 26.9 ± 1.6 wt.%. Hydrogels did not form in ddH2O with MEHQ and the polymer precipitated prior to gelation.

3.3.2. Degradation—The degradation profile of hydrogels was studied by measuring mass loss of lyophilized samples in PBS at 37 °C over a period of 9 weeks (Fig. 9A). Gels reached equilibrium within 48 h of incubation displaying a characteristic sol fraction of approximately 6 wt.%, similar to the value observed in equilibration studies. The hydrogel degraded linearly *in vitro* at a rate of 2 wt.% a week over the 9 weeks. Furthermore, the hydrogel displayed approximately constant polymer mass and volume fractions over the initial 4-week period with an increased solvent uptake apparent from 6 weeks (Fig. 9B). After 4 weeks the hydrogel exhibited a noticeable reduction in mechanical rigidity and could be easily compressed upon handling.

3.3.3. Mechanical testing—Tensile testing was performed on hydrogels cured at 37 °C in their initial and equilibrium-swollen states (Fig. 10). From the data obtained, ultimate tensile strengths and terminal extensions were recorded (Table 1). Elastomer rubber elasticity theory was applied to quantify the elastic modulus of the hydrogels by using the characteristic linear relationship between tensile stress and deformation factor over the extension ratio range of relevance [27]. For the equilibrated hydrogels a shear modulus of 63.26 ± 2.13 kPa was determined, which was significantly greater than the modulus recorded for the cured hydrogels, calculated to be 50.98 ± 1.42 kPa ($p << 0.001$). By assuming an isotropic material that behaves as a neo-Hookean incompressible solid, the elastic modulus, E was approximated to be 189.8 and 152.9 kPa for the equilibrated and cured gels respectively. Through the application of equation (3) and knowledge of the volume fraction parameters ($v_{2,r} = 0.221$, $v_{2,s} = 0.376$) the percentage of elastically effective chains was calculated to be approximately 11% of the total number of initial chains ($v_e \sim 0.021$ mol L^{-1}) and was consistent in both the cured and equilibrium states. The extent of reaction was calculated to be approximately 96.98% based on the theory of Miller-Macosko, but the number of elastically effective chains was overestimated to be 0.15 mol L^{-1} using this model. By taking the root mean squared value of the distance between crosslinks, the mesh size of the system was approximated at 7 nm and 6.9 nm in the cured and equilibrium states respectively.

3.4. Evaluation of drug delivery and tissue engineering applications in vitro

3.4.1. Release of methylprednisolone sodium succinate from the hydrogels—The degradation constant for MPSS in PBS was determined as $5.98 \pm 0.50 \times 10^{-3}$ h^{-1} by exponential regression ($R^2 = 0.997$, Fig. 11A). By solution of ordinary differential equations for mass transfer and degradation, the degradation constants in the gel and mass transfer coefficients were calculated by regression (Fig. 11B). The determined mass transfer coefficient was $1.54 \pm 0.29 \times 10^{-4}$ h^{-1} while the degradation constant for MPSS in the gels was $3.12 \pm 0.10 \times 10^{-3}$ h^{-1}. Using these two coefficients, the drug release was predicted for infinite sink conditions (Fig. 11C).

3.4.2. Cell adhesion mediated by peptide functionalization—Functionalization of hydrogels by incorporation of an oligolysine peptide (Cys-(Lys)14-Cys) was performed to promote cell adhesion on the hydrogels (Fig. 12). No cell attachment was observed for hydrogels with zero or 5 μg/mL Cys-(Lys)14-Cys. Attachment and process extension of cultured murine mesenchymal stem cells were observed for hydrogels containing 50 μg/mL, with a similar conformation to cells in uncoated wells. A concentration of 500 μg/ mL caused the cells to adhere to the gel but form spherical conformations without process extension.

4. Discussion

4.1. Thermodynamic considerations of ETTMP in PBS

Successful preparation of the hydrogels was found to be dependent on the solubility of the ETTMP in the solvent, which was shown to have a non-linear dependence on concentration in PBS at 4 °C (Fig. 2). In unsuccessful attempts, precipitation of the polymer at 37 °C

occurred during chemical reaction, resulting in incomplete conversion and a high sol fraction. Assessing the stability of ETTMP in PBS when heated from 4 to 37 °C provided a practically relevant indication of solubility throughout the gelation period at physiological temperature. It is well understood that polymers containing ethylene glycol units exhibit a concentration dependent lower critical solution temperature (LCST) [31]. Visible light absorbance data of ETTMP in PBS during heating was fitted to an error function, where the inflection point signifies 50% precipitation. Therefore, a characteristic error function was observed as the cumulative function when a lower critical solution temperature was reached and phase separation occurs [32]. The solubility of ETTMP in PBS appeared to be improved upon mixing with PEG-400-DA solution and was maintained throughout the complete gelation process as long as the mixture was maintained at 4 °C for the initial 5 min.

4.2. Physical chemistry of gelation mechanism

Understanding the timeline of hydrogel formation was of critical importance for determining its practical use as an injectable biomedical material. Dynamic rheological measurements were a convenient means of assessing the gelation kinetics of the hydrogel system and provided insight into the mechanism of gelation through the control of various gelation parameters such as pH, temperature and macromer stoichiometry [25,33]. The characteristic hydrogel formation response of the current system, as depicted in Fig. 6, can be described by standard branch gelation theory developed by Flory and Stockmayer [27,34].

The data presented in Fig. 7 provide support for a conjugate Michael addition reaction mechanism between a thiolate and the activated unsaturated carbon double bond of the acrylate. The gelation time, or reaction rate, was linearly dependent on the concentration of protons and corresponding thiolate anions in solution. While a pK_a of 9.87 indicates that a small proportion of thiol groups in ETTMP is dissociated in pH 7.4 PBS, thiolate anions will continue to be produced under rapid equilibration with their rate of consumption according to Le Châtelier's principle. The small variation in gelation time and physical properties with the inclusion of a radical inhibitor MEHQ in PBS indicated that a radical thiyl-acrylate reaction mechanism was not kinetically competitive with the addition mechanism. This is advantageous in the minimization of transient free radical production *in situ*, compared to approaches using photoinitiators and UV light.

4.3. Mechanical properties

The PEG-400-DA/ETTMP hydrogel exhibited a de-swelling property during equilibration at 37 °C. This can be attributed to the LCST of the PEG-based precursors. In addition, a relief of tension was observed, as the hydrogels were separated from the walls of their molds during removal, indicating residual tensile stress after curing. This characteristic makes it a candidate material for applications where pressure exerted by hydrogel swelling may cause severe nerve damage [14–17].

Biomaterials often require a resorbable capacity *in vivo* following the completion of their desired function so as to minimize the extent of the induced foreign body response. Poly(α-hydroxy esters) have been incorporated into the PEG-based system to increase the rate of hydrolytic degradation [35]. The PEG-DA-400/ETTMP system contains ester bonds,

allowing the material to resorb within an estimated 12-month *in vitro*. However, the *in vitro* experiment does not account for many factors *in vivo* such as enzymatic and phagocytic activity as well as mechanical loading, which may increase the degradation rate. Due to the hydrophilic nature of PEG, bulk degradation is the predominate mechanism [36]. The linear profile of the macroscopic degradation curve for the hydrogel as depicted in Fig. 9, may be attributed to the net result of two competing processes, namely first-order hydrolysis and crosslink density reduction, which are stochastic in nature [37].

The mechanical properties of biomaterials can influence the phenotype and activity of local and systemic cells, dictating foreign body and wound healing responses. The developed hydrogel displays a modulus of elasticity of 189.8 kPa that is comparable, in magnitude, to a range of soft human tissues. It is important to note that the material failed to obtain mechanical properties close to the affine or phantom values predicted by the Miller-Macosko model (Table 1). This was attributed to a significant difference in the number of elastically active chains actually incorporated (11% of the initial chains, $v_e = 0.021$ mol L^{-1}) compared to that the model prediction (82%, $v_a = 0.15$ mol L^{-1}). However, this is to be expected due to a number of factors such as low volume fraction of polymer during curing, the use of low molecular weight macromers and the possibility of intramolecular reactions, which may all contribute to non-ideal network formation.

4.4. Sustained drug release

MPSS is a glucocorticoid prodrug, with anti-inflammatory and immunosuppressant properties, that is currently a clinical treatment option for acute traumatic spinal cord injury [38]. However, high-dose intravenous administration immediately post-injury is being widely abandoned by neurosurgeons due to complications associated with systemic immunosuppression, including increased risk of pneumonia and sepsis [39]. MPSS has a half-life of 109 h in PBS at 37 °C. In aqueous media, the ester bond between the methylprednisolone and succinate hydrolyses, yielding free meth-ylprednisolone (MP) which has limited solubility in PBS due to its hydrophobic nature. MP was likely not detected by HPLC for this reason in drug release experiments. In future experiments, it may be possible to measure MP by extraction with organic solvents. The drug release experiment was modeled using a system of ordinary differential equations to include rates of mass transfer, proportional to the MPSS concentration difference between the hydrogel and the PBS, and drug degradation in both the hydrogel and PBS. Experimental data were fitted to the solutions to determine the mass transfer coefficient and degradation constants. The degradation rates of MPSS in the PBS and hydrogel were modeled separately in the differential equations to assess whether encapsulation had a stabilizing effect on the active life of the drug. Regression analysis using the solution to the system of equations identified a lower degradation constant for MPSS in the hydrogel, suggesting that the material may create a protective environment that transiently impedes drug degradation. To predict the actual release profile of methylprednisolone in vivo, the equations were modified for an infinite sink and resolved using the determined constants. In reality, the sink conditions in vivo will deviate from this infinite sink approximation. A more accurate mathematical description would need to consider further the spatial dimensions of the system, account for interstitial diffusion and convection, as well as make concession for receptor binding and

other biological processes. The hydrolysis of MPSS to MP once it has been released from the hydrogel is of little concern for local release systems as MP is the active form of the steroid and the limited aqueous solubility will not hinder activity. A key feature of the MPSS release profile from the current system is that the release time period is independent of the initial concentration in the hydrogel. For biomedical applications, this means that the drug dosage could be tailored to individual patients without increasing the volume of the drug depot required to administer it locally over a precise period of time.

4.5. Functionalization and cell adhesion

Whilst PEG is generally favored in biomedical applications because of limited protein adsorption, this can result in limited interaction with cells. To improve cell interactions, the hydrogel can be functionalized with peptides. One advantage of the PEG-DA-400/ETTMP hydrogel is that it involves thiol chemistry, which can be exploited to attach almost any compound with a thiol group, including any peptide containing cysteine to promote a specific cell response. Incorporation of an oligolysine peptide into the hydrogel promoted surface attachment of mMSCs in a concentration dependent manner *in vitro*. Polylysine was chosen as an initial proof of concept as it generally promotes cell adhesion, and in fact is used to promote neural stem cell attachment to culture plates [40,41]. Others have shown that cell attachment on PEG-based hydrogels can also be achieved using short peptide sequences from extracellular matrix proteins [42,43]. The current nanoscale mesh size of the hydrogel (~6.9 nm) was too small for cellular ingrowth into the material. However, the small mesh size is advantageous for the characteristic de-swelling and drug release properties. Furthermore, a small mesh size may be useful to isolate encapsulated cells from a host immune system to prevent rejection. Recently, others have demonstrated incorporation of macroscopic pores or channels into similar hydrogels for cell ingrowth using sacrificial substrates of fibrin or poly(a-hydroxy esters) [44,45]. However, utilizing these approaches would not preserve injectability. Future work towards use of this hydrogel in regenerative medicine will therefore focus on the development of procedures to create macroporous structures with controlled architecture in situ following injection and gelation.

5. Conclusion

This paper presents the rational design of a hydrogel, seeking to address the engineering challenges associated with clinical translation of injectable in situ gelling biomaterials. This poly(ethylene glycol)-based hydrogel crosslinked in aqueous media via conjugate Michael addition reaction of thiol and acrylate groups, resulting in nearly complete conversion and minimal sol fraction. By selecting low molecular weights macromer precursors with favorable solvent interactions the hydrogel exhibited syneresis under simulated physiological conditions in vitro. The suitability of the material for sustained release of a hydrophilic small molecule drug, methylprednisolone sodium succinate, was demonstrated with high encapsulation efficiency and programmable dosage which facilitated release over a concentration independent timeline. Furthermore, incorporation of an oligolysine peptide promoted concentration dependent adhesion of murine mesenchymal stem cells in vitro.

Acknowledgments

We thank Dr. Arthur J. Coury (Boston, MA) for reviewing the manuscript and engaging in discussions. C.D.P. was supported by the MIT/CIMIT Medical Engineering Fellowship. T.M.O was supported by the General Sir John Monash Award. This research was sponsored by a gift to MIT by InVivo Therapeutics Corporation. This research was sponsored by the Armed Forces Institute of Regenerative Medicine award number W81XWH-08-2-0034. The U.S. Army Medical Research Acquisition Activity, 820 Chandler Street, Fort Detrick MD 21702-5014 is the awarding and administering acquisition office. The content of the manuscript does not necessarily reflect the position or the policy of the Government, and no official endorsement should be inferred.

Role of the funding source

InVivo Therapeutics Corporation provided assistance determining the general design of this study to develop a injectable hydrogel.

References

1. Drury JL, Mooney DJ. Hydrogels for tissue engineering: scaffold design variables and applications. Biomaterials. 2003; 24(24):4337–4351. [PubMed: 12922147]
2. Lin C-C, Anseth K. Peg hydrogels for the controlled release of biomolecules in regenerative medicine. Pharm Res. 2009; 26(3):631–643. [PubMed: 19089601]
3. Slaughter BV, Khurshid SS, Omar ZF, Khademhosseini A, Peppas NA. Hydrogels in regenerative medicine. Adv Mater. 2009; 21(32–33):3307–3329. [PubMed: 20882499]
4. Chapman RG, Ostuni E, Liang MN, Meluleni G, Kim E, Yan L, et al. Polymeric thin films that resist the adsorption of proteins and the adhesion of bacteria. Langmuir. 2001; 17(4):1225–1233.
5. Pathak CP, Sawhney AS, Hubbell JA. Rapid photopolymerization of immuno-protective gels in contact with cells and tissue. J Am Chem Soc. 1992; 114(21):8311–8312.
6. Salinas CN, Anseth KS. Mixed mode thiol-acrylate photopolymerizations for the synthesis of peg-peptide hydrogels. Macromolecules. 2008; 41(16):6019–6026.
7. Rydholm AE, Bowman CN, Anseth KS. Degradable thiol-acrylate photopolymers: polymerization and degradation behavior of an in situ forming biomaterial. Biomaterials. 2005; 26(22):4495–4506. [PubMed: 15722118]
8. Lee TY, Roper TM, Jonsson ESn, Guymon CA, Hoyle CE. Thiol-ene photo-polymerization kinetics of vinyl acrylate/multifunctional thiol mixtures. Macromolecules. 2004; 37(10):3606–3613.
9. DeForest CA, Polizzotti BD, Anseth KS. Sequential click reactions for synthesizing and patterning three-dimensional cell microenvironments. Nat Mater. 2009; 8:659–664. [PubMed: 19543279]
10. Lutolf MP, Hubbell JA. Synthesis and physicochemical characterization of end-linked poly(ethylene glycol)-co-peptide hydrogels formed by michael-type addition. Biomacromolecules. 2003; 4(3):713–722. [PubMed: 12741789]
11. Elbert DL, Pratt AB, Lutolf MP, Halstenberg S, Hubbell JA. Protein delivery from materials formed by self-selective conjugate addition reactions. J Control Release. 2001; 76(1–2):11–25. [PubMed: 11532309]
12. Cushing MC, Anseth KS. Materials science: hydrogel cell cultures. Science. 2007; 316(5828): 1133–1134. [PubMed: 17525324]
13. Sawhney AS, Pathak CP, Hubbell JA. Bioerodible hydrogels based on photo-polymerized poly(ethylene glycol)-co-poly(alpha-hydroxy acid) diacrylate macromers. Macromolecules. 1993; 26(4):581–587.
14. Thavarajah DM, De Lacy PM, Hussain RM, Redfern RMF. Postoperative cervical cord compression induced by hydrogel (duraseal): a possible complication. Spine. 35(1):E25–E26. [PubMed: 20042944]
15. Blackburn, Sl; Smyth, MD. Hydrogel-induced cervicomedullary compression after posterior fossa decompression for chiari malformation. J Neurosurg Pediatr. 2007; 106(4):302–304.
16. Roldan-Pallares M, del Castillo Sanz JL, Awad-El Susi S, Refojo MF. Long-term complications of silicone and hydrogel explants in retinal reattachment surgery. Arch Ophthalmol. 1999; 117(2): 197–201. [PubMed: 10037564]

17. Hwang KI, Lim JI. Hydrogel explant fragmentation 10 years after scleral buckling surgery. Arch Ophthalmol. 1997; 115(9):1205–1206. [PubMed: 9298070]
18. Bakshi A, Fisher O, Dagci T, Himes BT, Fischer I, Lowman A. Mechanically engineered hydrogel scaffolds for axonal growth and angiogenesis after transplantation in spinal cord injury. J Neurosurg Spine. 2009; 1(3):322–329. [PubMed: 15478371]
19. Pathak CP, Barman SP, Philbrook MC, Sawhney AS, Coury AJ, Avila LZ, et al. Multiblock biodegradable hydrogels for drug delivery and tissue treatment. 2001 US patent no. 0072961.
20. Klimo P Jr, Khalil A, Slotkin JR, Smith ER, Scott RM, Goumnerova LC. Wound complications associated with the use of bovine serum albumin-glutaralde-hyde surgical adhesive in pediatric patients. Neurosurgery. 2007; 60(4):305–309. [PubMed: 17415167]
21. Metters A, Hubbell J. Network formation and degradation behavior of hydrogels formed by michael-type addition reactions. Biomacromolecules. 2004; 6(1):290–301. [PubMed: 15638532]
22. Lowe AB. Thiol-ene “click” reactions and recent applications in polymer and materials synthesis. Polym Chem. 2010; 1:17–36.
23. Mather BD, Viswanathan K, Miller KM, Long TE. Michael addition reactions in macromolecular design for emerging technologies. Prog Polym Sci. 2006; 31(5):487–531.
24. Smith MD. High-performance liquid chromatographic determination of hydrocortisone and methylprednisolone and their hemisuccinate esters in human serum. J Chromatogr B. 1979; 164(2):129–137.
25. Chambon F, Winter HH. Linear viscoelasticity at the gel point of a crosslinking pdms with imbalanced stoichiometry. J Rheol. 1987; 31(8):683–697.
26. Winter HH. Can the gel point of a cross-linking polymer be detected by the g’ – g” crossover? Polym Eng Sci. 1987; 27(22):1698–1702.
27. Flory, PJ. Ithaca. N.Y: Cornell University Press; 1953. Principles of polymer chemistry.
28. Treloar, LRG. 2d ed.. Oxford: Clarendon Press; 1958. The physics of rubber elasticity.
29. Gnanou Y, Hild G, Rempp P. Molecular structure and elastic behavior of poly (ethylene oxide) networks swollen to equilibrium. Macromolecules. 1987; 20(7):1662–1671.
30. Miller DR, Macosko CW. A new derivation of post gel properties of network polymers. Macromolecules. 1976; 9(2):206–211.
31. Kjellander R, Florin E. Water structure and changes in thermal stability of the system poly(ethylene oxide)ewater. J Chem Soc Faraday Trans. 1981; 77(9)
32. Barnes MD, Ng KC, Fukui K, Sumpter BG, Noid DW. Probing phase-separation behavior in polymer-blend microparticles: effects of particle size and polymer mobility. Macromolecules. 1999; 32(21):718–719.
33. Chiou B-S, English RJ, Khan SA. Rheology and photo-cross-linking of thiol-ene polymers. Macromolecules. 1996; 29(16):5368–5374.
34. Stockmayer WH. Theory of molecular size distribution and gel formation in branched-chain polymers. J Chem Phys. 1943; 11(2):45–55.
35. West JL, Hubbell JA. Photopolymerized hydrogel materials for drug delivery applications. React Polym. 1995; 25(2e3):139–147.
36. Sawhney AS, Pathak CP, Hubbell JA. Bioerodible hydrogels based on photo-polymerized poly(ethylene glycol)-co-poly(a-hydroxy acid) diacrylate mac-romers. Macromolecules. 1993; 26(4):581–587.
37. Metters AT, Anseth KS, Bowman CN. Fundamental studies of a novel, biodegradable peg-b-pla hydrogel. Polymer. 2000; 41(11):3993–4004.
38. Bracken MB, Shepard MJ, Collins WF, Holford TR, Young W, Baskin DS, et al. A randomized controlled trial of methylprednisolone or naloxone in the treatment of acute spinal-cord injury Results of the Second National Acute Spinal Cord Injury Study. N Engl J Med. 1990; 322(20): 1405–1411. [PubMed: 2278545]
39. Hugenholtz H. Methylprednisolone for acute spinal cord injury: not a standard of care. Can Med Assoc J. 2003; 168(9):1145–1146. [PubMed: 12719318]
40. Yavin E, Yavin Z. Attachment and culture of dissociated cells from rat embryo cerebral hemispheres on polylysine-coated surface. J Cell Biol. 1974; 62(2):540–546. [PubMed: 4609989]

41. Banker GA, Cowan WM. Rat hippocampal neurons in dispersed cell culture. Brain Res. 1977; 126(3):397–425. [PubMed: 861729]

42. Burdick JA, Anseth KS. Photoencapsulation of osteoblasts in injectable rgd-modified peg hydrogels for bone tissue engineering. Biomaterials. 2002; 23(22):4315–4323. [PubMed: 12219821]

43. Lutolf MP, Lauer-Fields JL, Schmoekel HG, Metters AT, Weber FE, Fields GB, et al. Synthetic matrix metalloproteinase-sensitive hydrogels for the conduction of tissue regeneration: engineering cell-invasion characteristics. P Natl Acad Sci U S A. 2003; 100(9):5413–5418.

44. Ford MC, Bertram JP, Hynes SR, Michaud M, Li Q, Young M, et al. A macro-porous hydrogel for the coculture of neural progenitor and endothelial cells to form functional vascular networks in vivo. P Natl Acad Sci U S A. 2006; 103(8):2512–2517.

45. Namba RM, Cole AA, Bjugstad KB, Mahoney MJ. Development of porous peg hydrogels that enable efficient, uniform cell-seeding and permit early neural process extension. Acta Biomater. 2009; 5(6):1884–1897. [PubMed: 19250891]

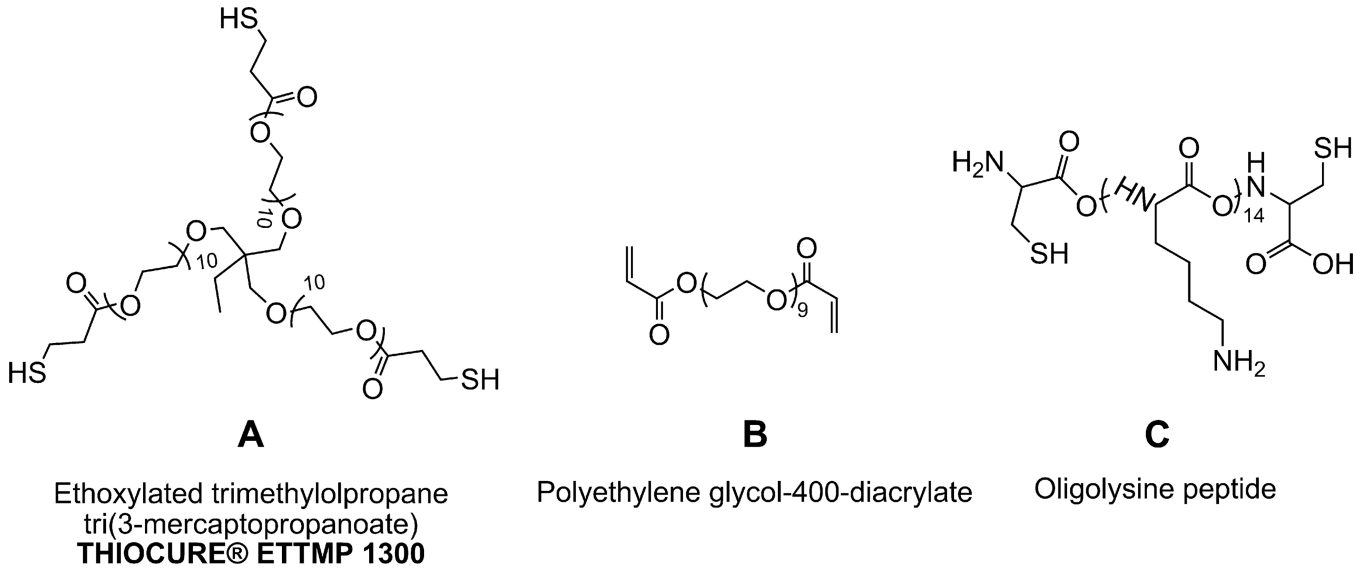

Fig. 1.

Hydrogel polymer components. (A) Ethoxylated trimethylolpropane tri(3-mercaptopropanoate) (ETTMP). (B) Poly(ethylene glycol) diacrylate (PEG-400-DA). (C) Oligolysine peptide with cysteine residues at N and C termini (Cys-$(Lys)_{14}$-Cys).

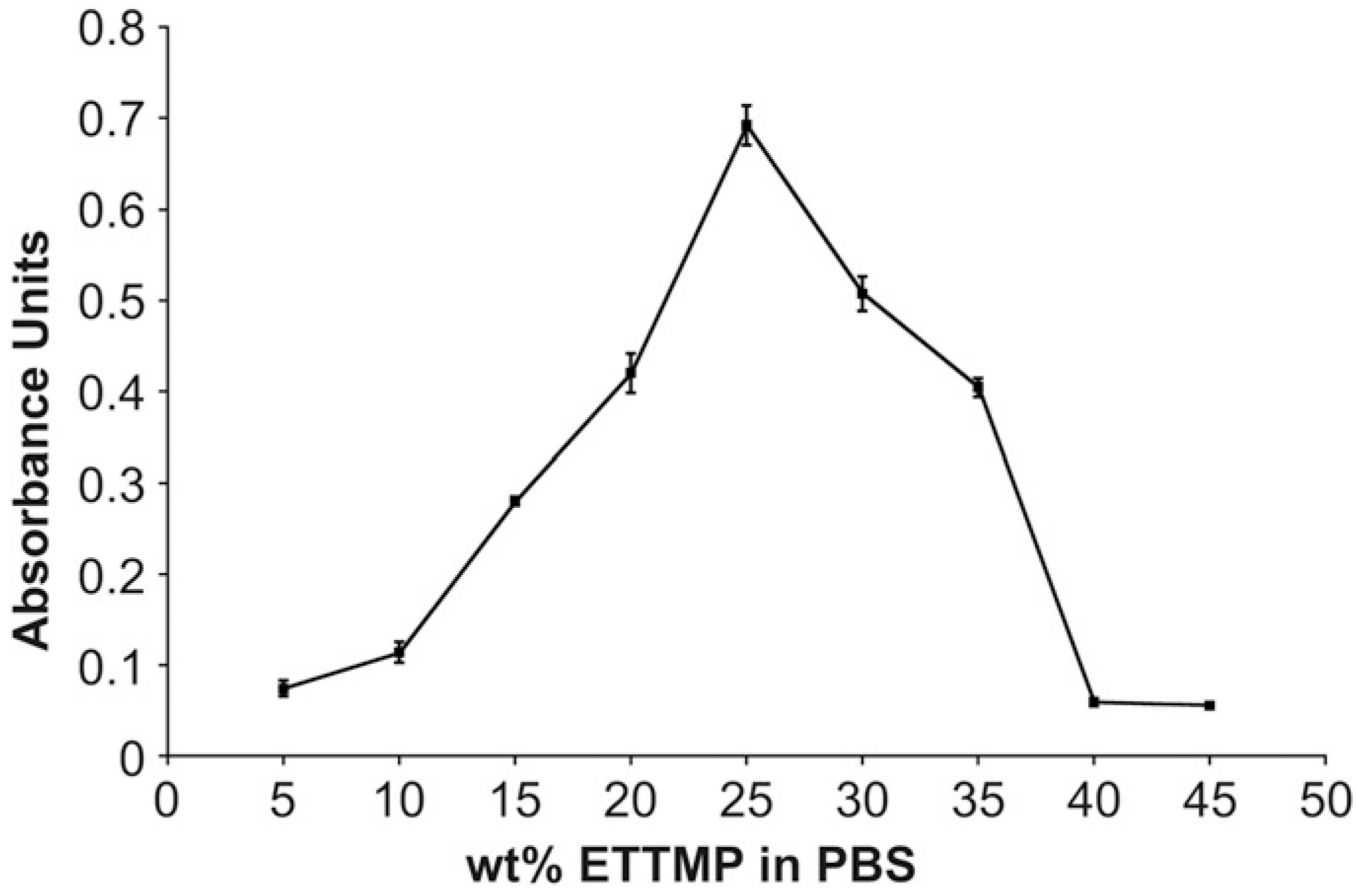

Fig. 2.

Solubility of ETTMP in PBS at 4 °C. The absorbances of 200 μL standards of ETTMP at different concentrations in PBS were measured at a wavelength of 450 nm. The dependence of solubility on concentration between 5 and 45 wt.% is not mono-tonic, with the solubility minimum observed at 25 wt.%. Error bars are standard deviation, $n = 4$.

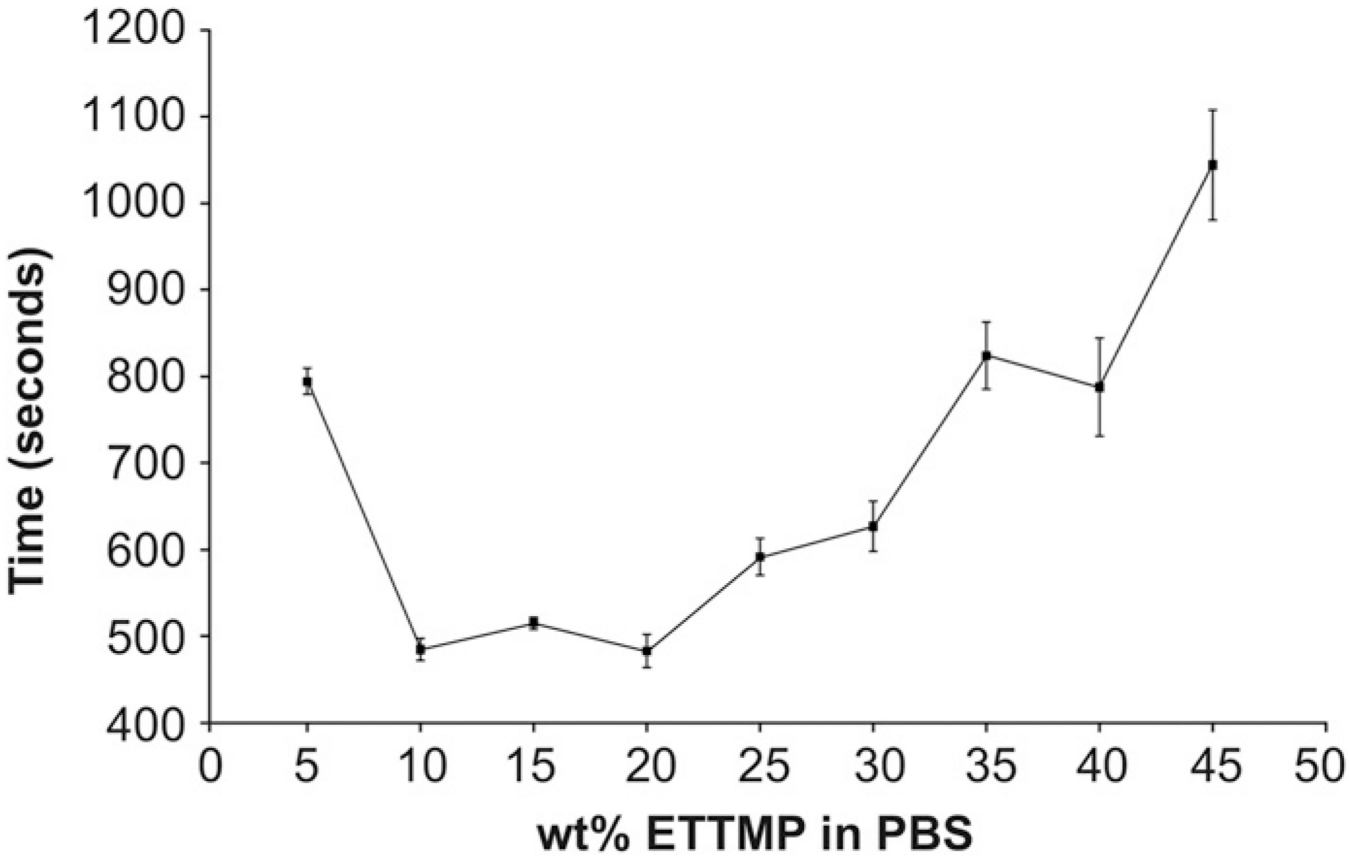

Fig. 3.

Stability of ETTMP in PBS from 4 °C to 37 °C. The absorbances of 200 μL standards of ETTMP at different concentration, prepared at 4 °C, were measured at a wavelength of 450 nm at 37 °C for 20 min. The graph shows the time taken for the standards to reach an inflection point in absorbance increase. The precipitation time is not a monotonic function of concentration between 5 and 45 wt.%, and is a maximum at 45 wt.%. Error bars are standard deviation, $n = 4$.

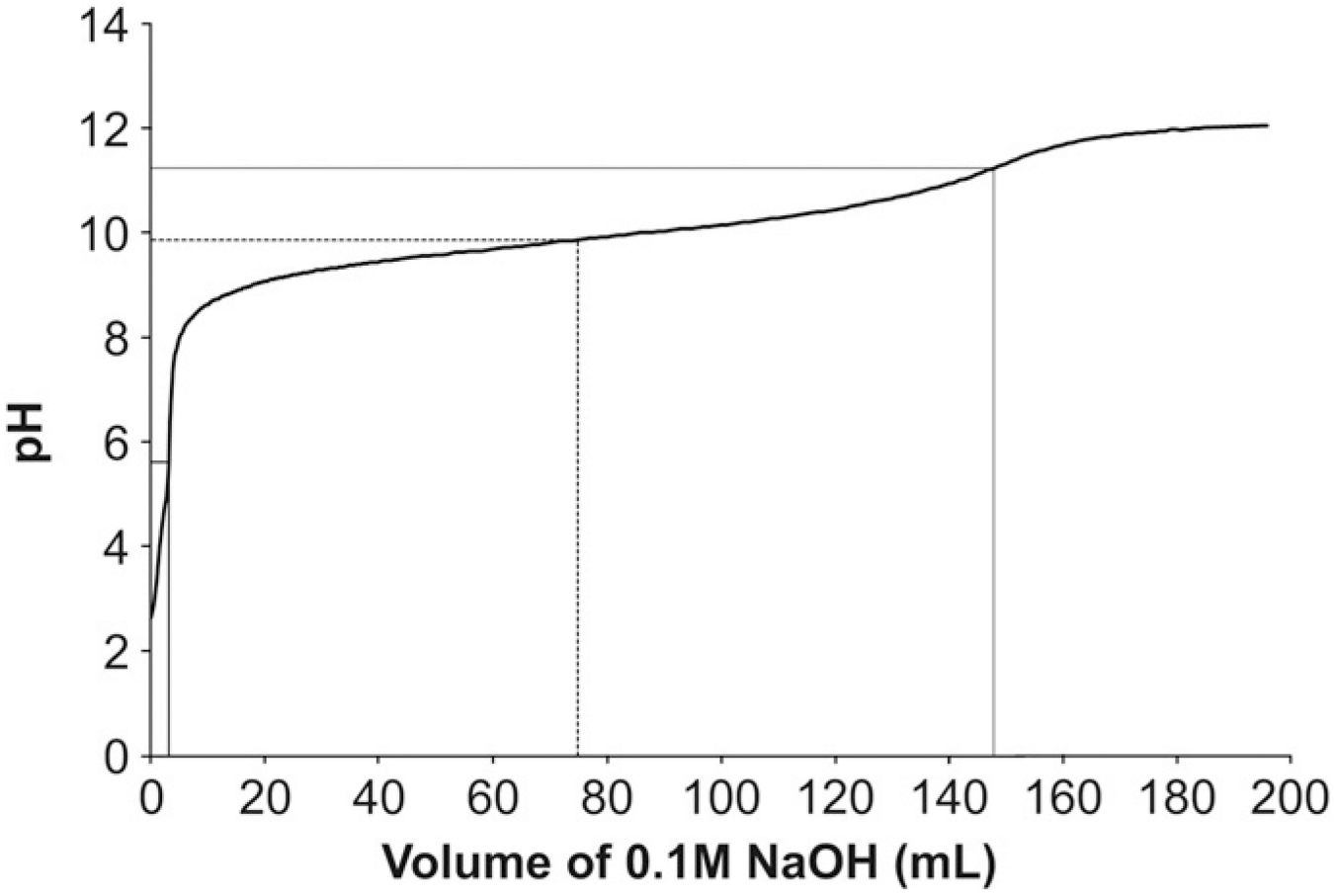

Fig. 4.

pK_a of ETTMP at 24 °C. 0.1 M ETTMP (0.3 N, 50 mL) at 24 °C was titrated with 0.1 M sodium hydroxide (NaOH) (0.1 N, 200 mL). The pK_a (dashed line) of 9.87 (74.8 mL 0.1 M NaOH) was determined as halfway between equivalence points (solid lines) at pH 5.62 (3.2 mL 0.1 M NaOH) and pH 11.23 (147.8 mL 0.1 M NaOH).

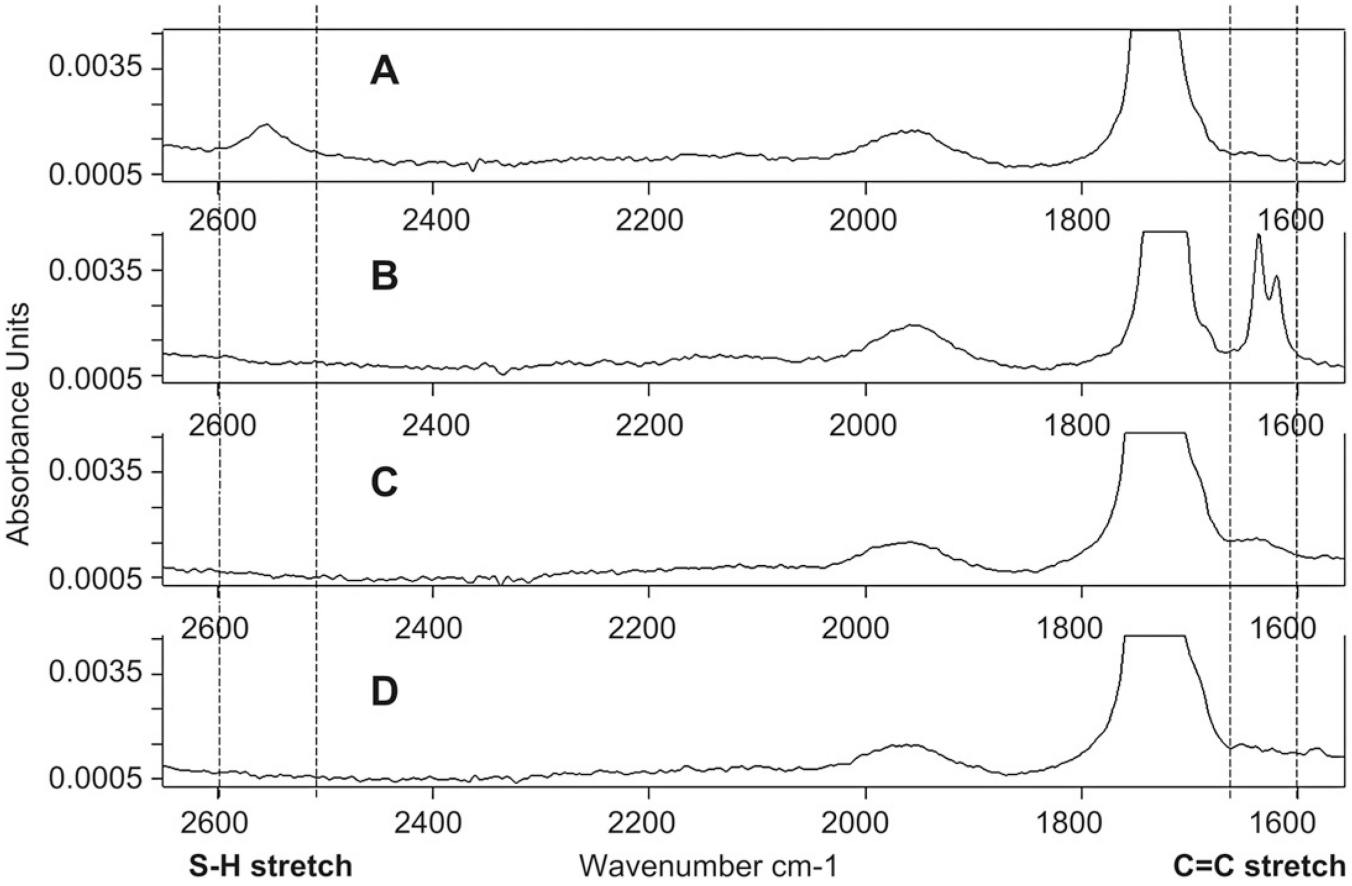

Fig. 5.

Fourier transform infrared spectroscopy (FT-IR) spectra, measured by attenuated total reflection through a Zinc Selenide (ZnSe) crystal, normalized by maximum and minimum absorbance. C=C stretch was measured at 1675—1600 cm^{-1} and S—H stretch at 2550–2600 cm^{-1}. (A) ETTMP. There is an S—H stretch but no C=C stretch. (B) PEG-400-DA. No S—H stretch is present but two peaks in the C=C stretch region are visible. (C) Hydrogel, cured and lyophilized. Following reaction of ETTMP and PEG-400-DA in PBS, both S—H stretch and C=C stretch have disappeared from the lyophilized network. (D) Hydrogel, equilibrated for 48 h and lyophilized. Spectrum displays same characteristics as the cured samples.

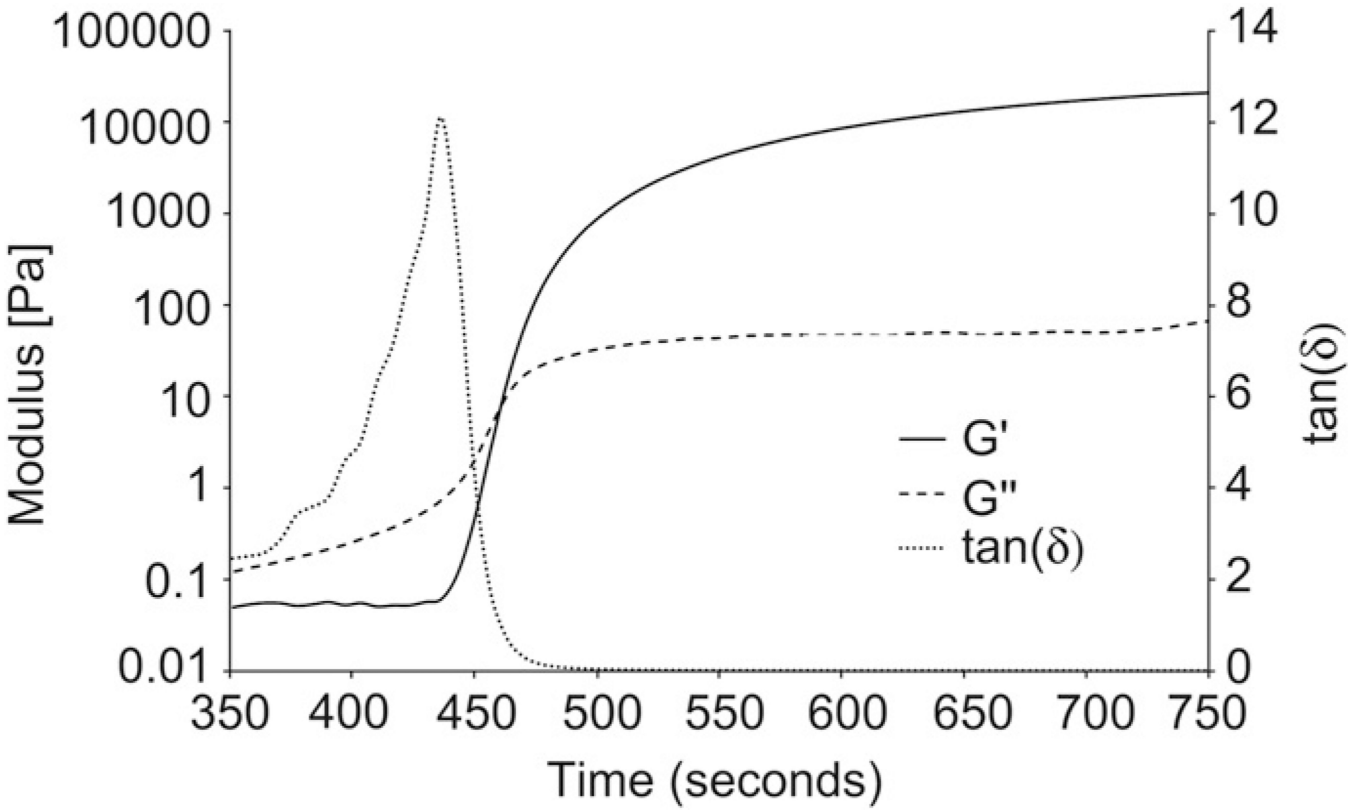

Fig. 6.

Dynamic rheology of characteristic gel point between ETTMP and PEG-400-DA in PBS. Gel point can be observed by dynamic rheology as the point where the magnitude of the elastic modulus (*G*') equals the loss modulus (*G*"). Shortly before this point, *G*" rises as the molecular weight of co-polymer chains increases significantly prior to network formation, resulting in increased viscosity. This is reflected in a maximum in tan(δ). At the gel point *G*' increases sharply as an infinite molecular weight network forms in solution. *G*' and *G*" reach asymptotes following complete conversion indicating a viscoelastic product.

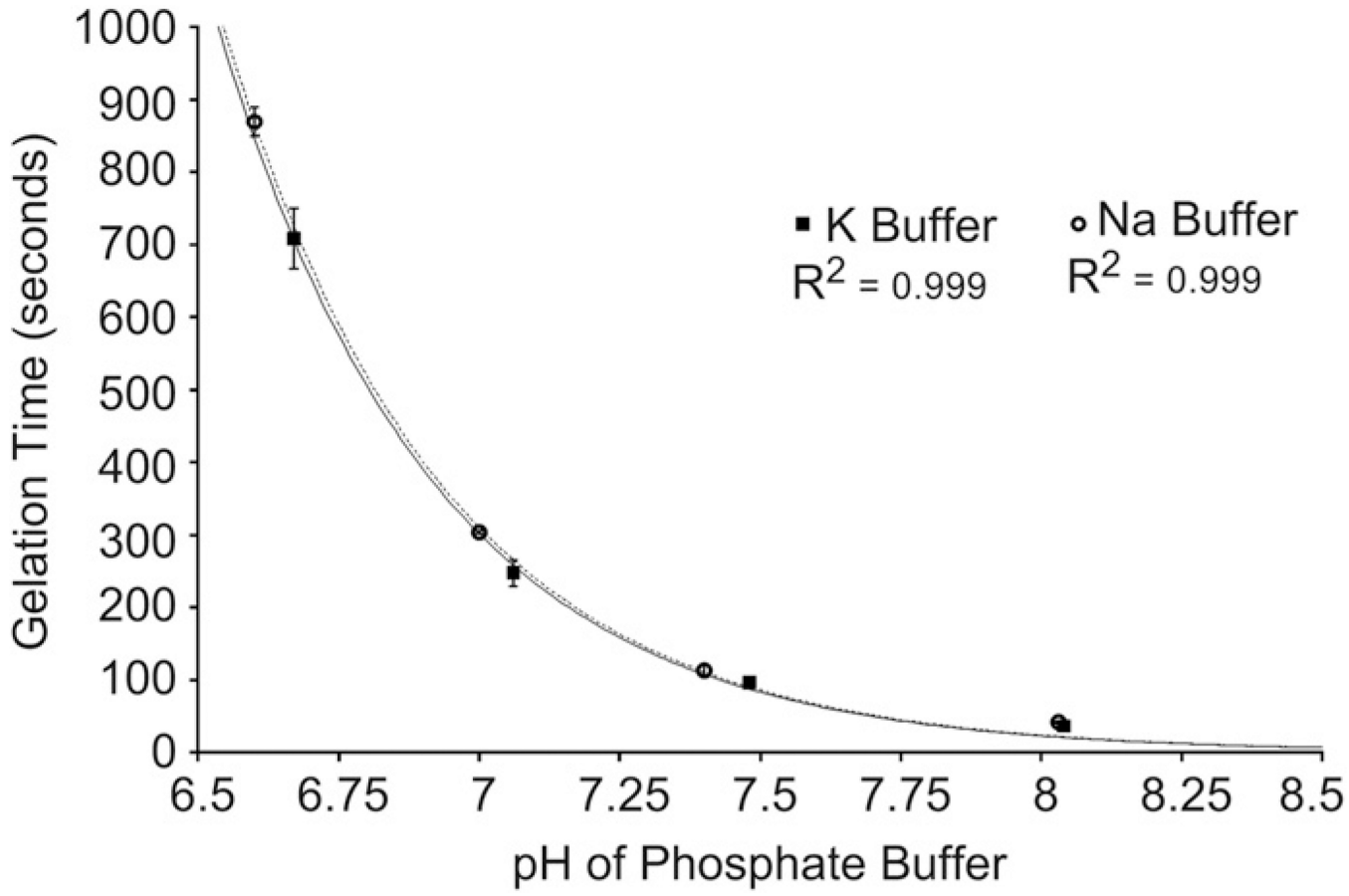

Fig. 7.

Gelation kinetics as a function of pH and alkali metal cation in 0.1 M phosphate buffer at 25 °C Gel point was determined by dynamic rheology where the magnitudes of elastic (*G*') and loss (*G*") moduli are equal. The reaction rate between ETTMP and PEG-400-DA follows an exponential dependence on buffer pH, and is therefore linearly proportional to thiolate concentration. The reaction rate is weakly dependent on the alkali metal cation in the buffer.

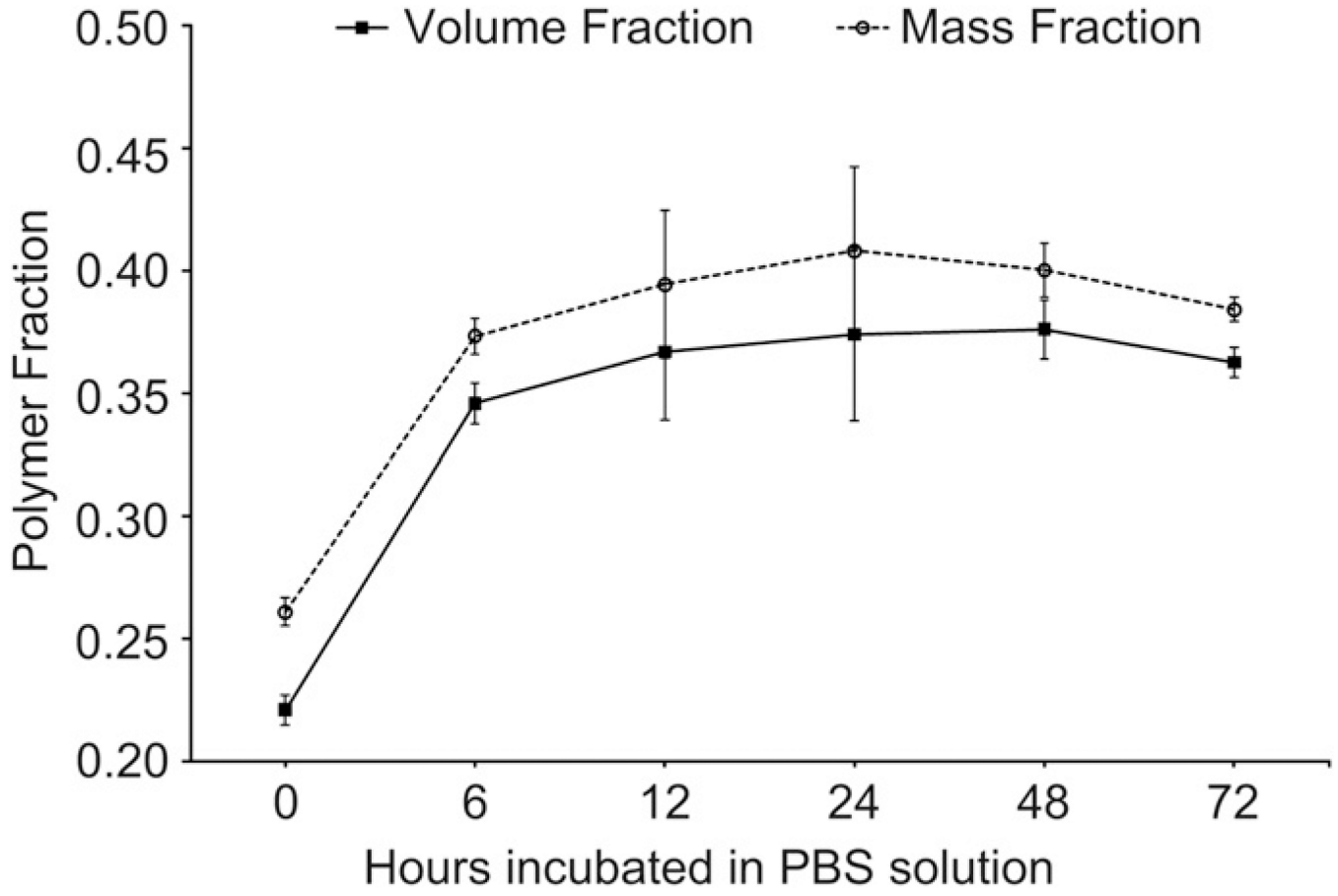

Fig. 8.

Equilibrium volume and mass fractions of hydrogels in PBS (pH 7.4) at 37 °C over a 72 h period. A rapid increase from the relaxed volume fraction is observed over the first 12 h before a stable equilibrium volume fraction is obtained and sustained at a near constant value over 48 h. The mass fraction profile traces the volume fraction response but is offset by 2—3% for each time point.

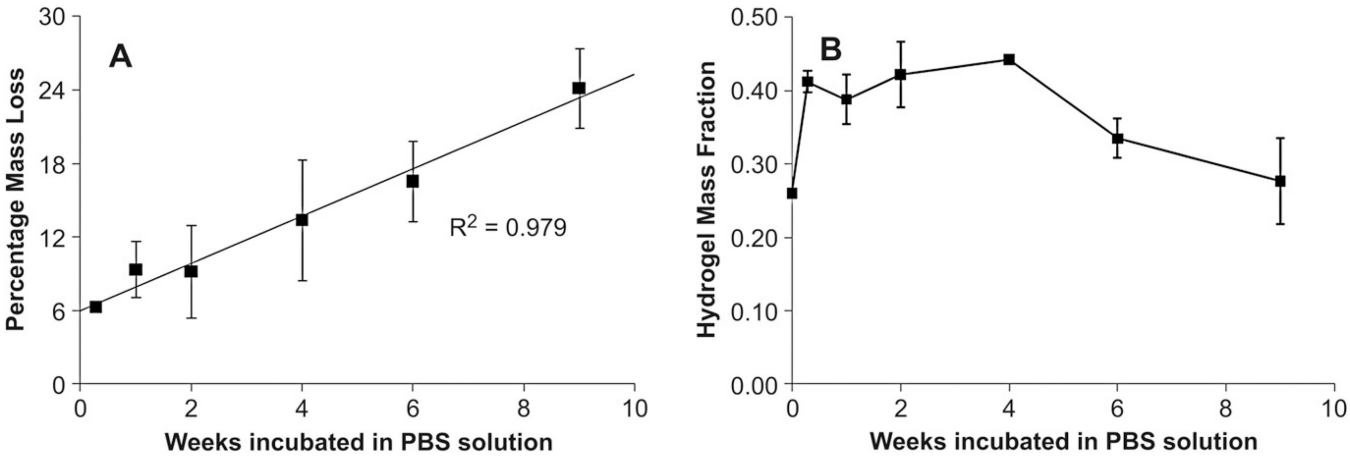

Fig. 9.

Degradation of hydrogels in PBS(pH 7.4) at 37 °C. The chosen buffer and temperature simulate physiological conditions where hydrolysis of ester bonds in the network result in gel mass loss. (A) Gels reach equilibrium within 48 h of incubation with no appreciable mass loss and degrade linearly over 9 weeks *in vitro*. (B) The polymer mass fraction remained approximately constant following equilibration for the first 4 weeks of incubation and exhibited increased solvent uptake from 6 weeks. Error is standard deviation, $n = 3$ for each time point.

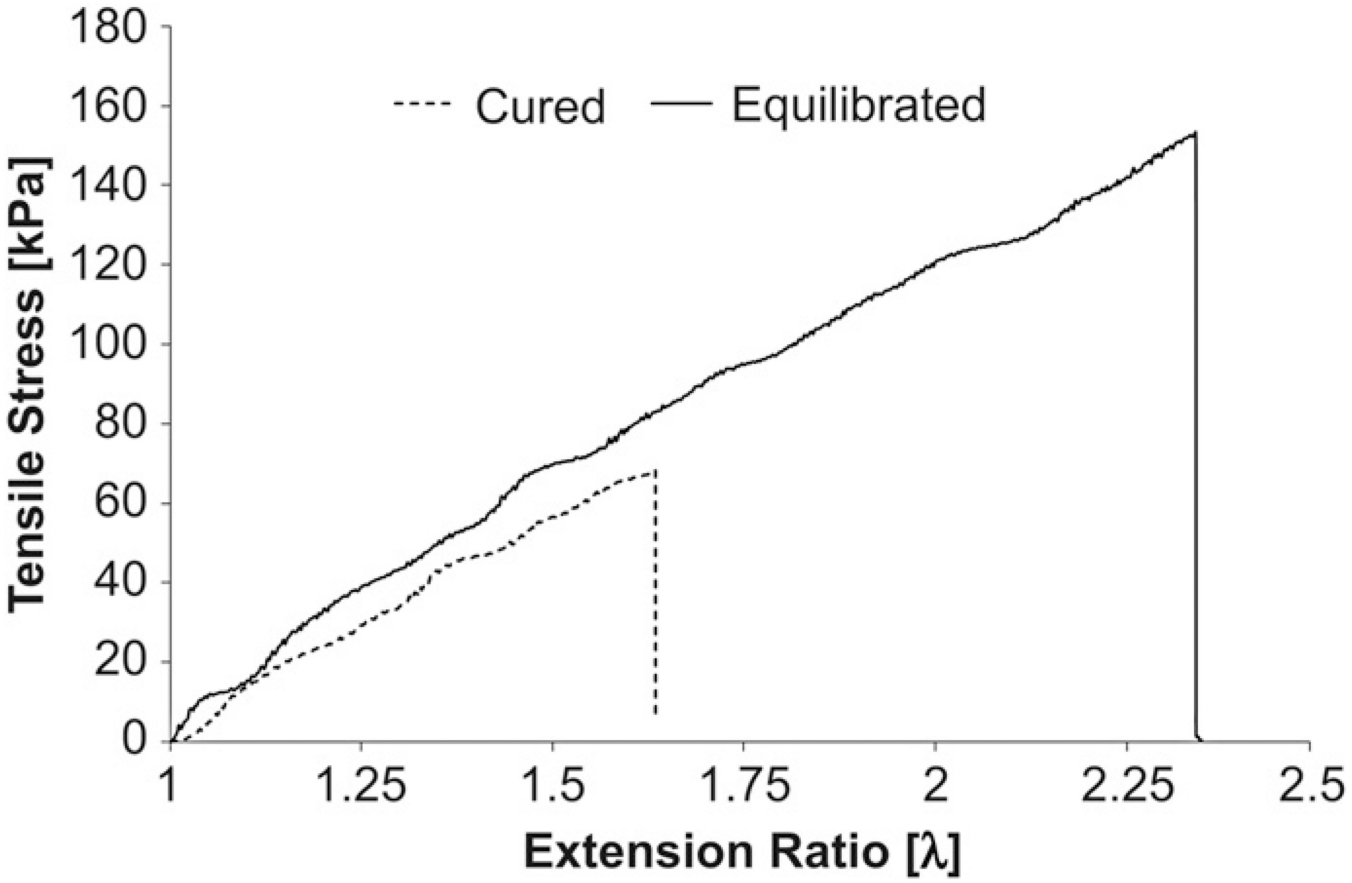

Fig. 10.

Tensile testing of hydrogels. Graph shows tensile stress versus extension ratio for cured and equilibrated hydrogels. Sample curves are shown for specimens that displayed median terminal elongation for each type.

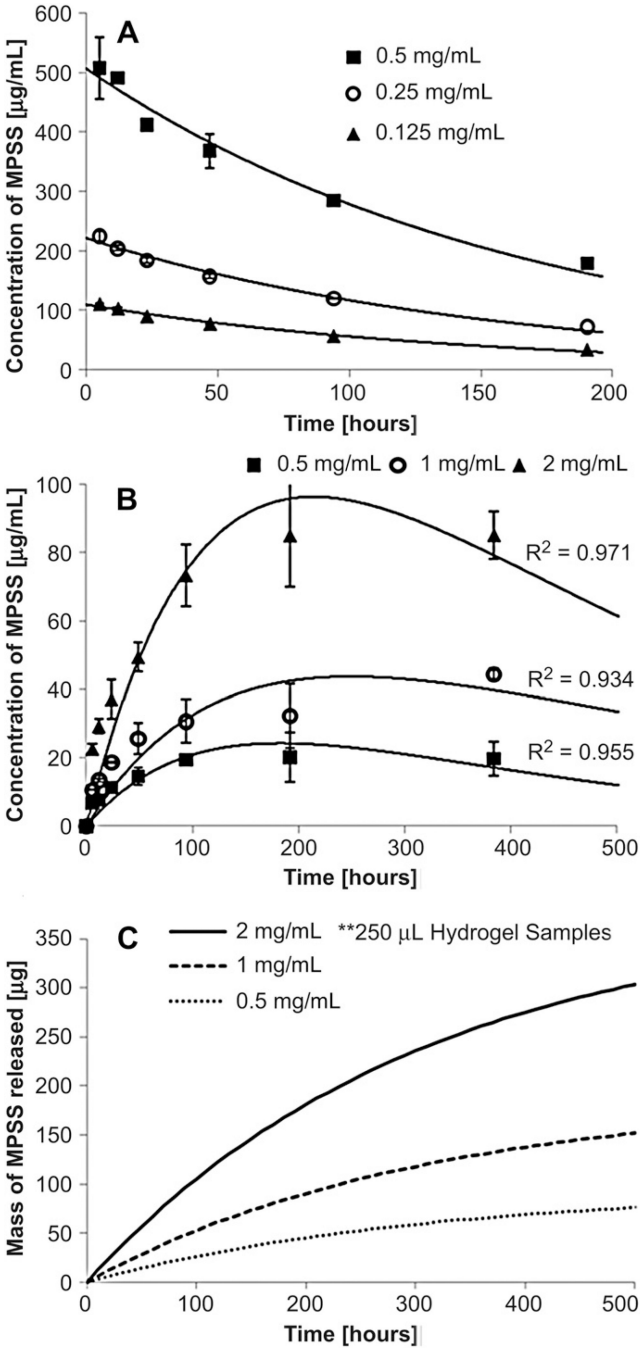

Fig. 11.

Controlled release of Methylprednisolone Sodium Succinnate (MPSS) from hydrogels in PBS (pH 7.4) at 37 °C. (A) Degradation of MPSS in PBS for three concentrations (0.125, 0.25 and 0.5 mg/mL). (B) Release profile of MPSS from hydrogels for three concentrations (0.5, 1, and 2 mg/mL). Graph displays experimental data for the release into PBS, including degradation of MPSS. $n = 3$ for each time point and concentration. (C) Predicted drug release from the hydrogels into an infinite sink, corrected for degradation of MPSS in PBS.

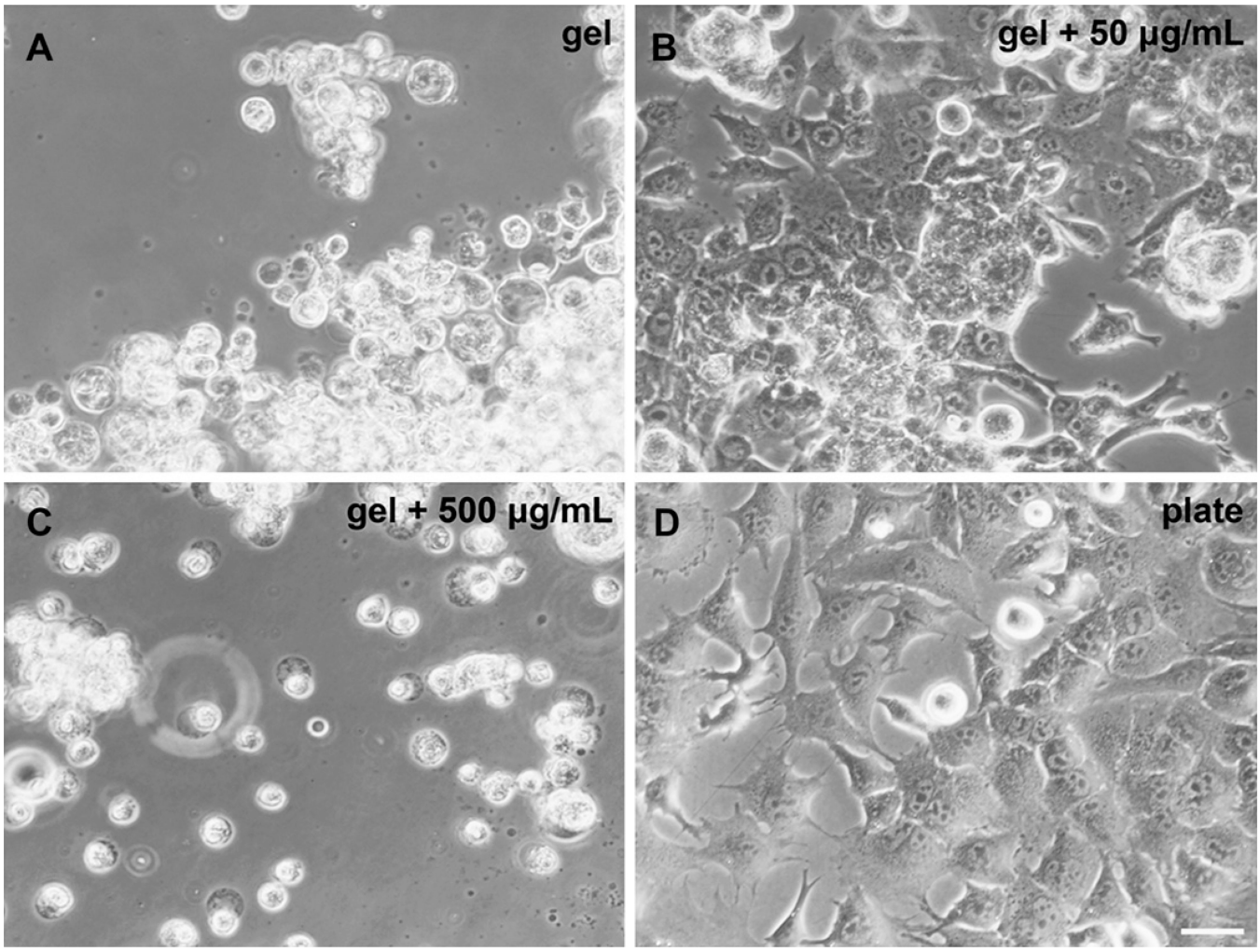

Fig. 12.

Functionalization of hydrogels to promote cell adhesion. 24-well polystyrene tissue culture plate was coated with 200 µL 25 wt.% thiol-acrylate hydrogels cured in 1XPBS (solvent exchanged to 1 × DMEM medium just prior to testing) containing Cys-(Lys)14-Cys at different concentrations (A, B, C) or wells left untreated (D). Murine mesenchymal stem cells (mMSC) were seeded 10^5 cells per well. 40× Phase 2 contrast light microscope images, 24 h post-seeding. Hydrogels containing 50 µg/mL promotes mMSC adhesion and process extension. $n = 4$ for each group.

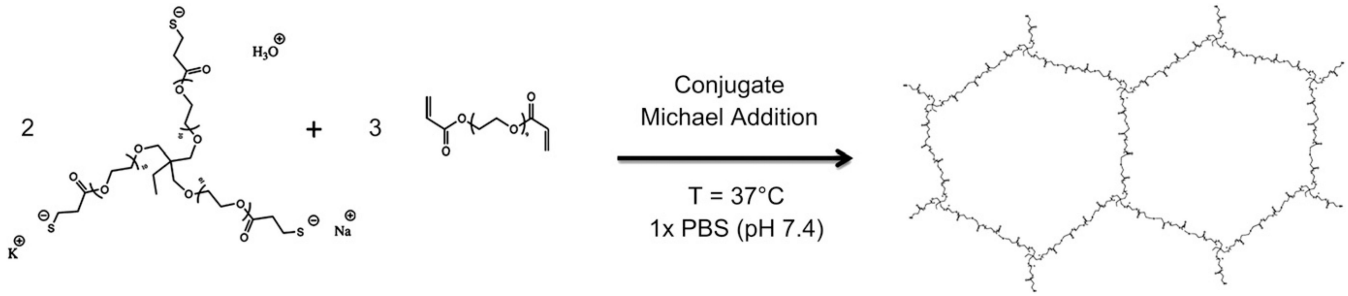

Scheme 1.

Formation of crosslinked network under physiological conditions. In aqueous medium a thiol functional group of ETTMP is in equilibrium with thiolate, its conjugate base. A 2:3 ratio of ETTMP and PEG-400-DA results in stoichiometric equivalents of thiol and acrylate functional groups. Due to the multi-functionality (n = 3) of ETTMP, a crosslinked network is formed. The thiolate anion in ETTMP attacks from the unsaturated β-carbon of the acrylate in PEG-400-DA, which is activated towards nucleophiles, in a nucleophilic conjugate addition reaction. In a buffer, a metal cation may act as a counterion to thiolate and as a Lewis acid, coordinating with the ester carbonyl in PEG-400-DA to further activate it, and promote nucleophilic attack of thiolate from the unsaturated β-carbon.

Table 1

Mechanical properties of hydrogels. Collated data from tensile tests on cured and equilibrated hydrogels are compared with calculated ideal values for Affine and Phantom network models derived from Miller-Macosko theory using the experimentally determined sol fraction. Erroris standard deviation, $n = 4$ for cured gels, $n = 6$ for swollen gels.

Hydrogel type	Shear modulus (G) [kPa]	Elastic modulus (E) [kPa]	Ideal shear moduli (affine and phantom models) [kPa]	Ultimate tensile strength [kPa]	Terminal extension factor (λ)
Cured ($n = 4$)	50.98 ± 1.42	152.9 ± 2.5	382.1 and 127.4	66.8 ± 6.9	1.637 ± 0.067
Equilibrated ($n = 6$)	63.26 ± 2.13	189.8 ± 3.7	456.2 and 152.1	141.7 ± 21.2	2.232 ± 0.220